Scalable Two-Mode 3-Port and 4-Port Mode Insensitive Silicon Photonic Switches

Alok Das, Guowu Zhang, *Graduate Student Member, IEEE*, Hassan Rahbardar Mojaver, *Member, IEEE*, and Odile Liboiron-Ladouceur, *Senior Member, IEEE*

***Abstract*— We propose and experimentally demonstrate a novel design approach for scalable 3-port and 4-port mode insensitive multimode switching matrices for the first two quasi-transverse electric (TE) modes. The mode insensitive phase shifter ensures less power consumption for simultaneous multimode signal transmission in a mode division multiplexing (MDM) network. At 1550 nm, the 3-port switch exhibits approximately 2.6 dB and 3.3 dB insertion loss for the longest path with a crosstalk of at most 10 dB and 8 dB over a bandwidth of 40 nm (1530 nm to 1570 nm) for TE_0 and TE_1 modes, respectively. The insertion loss measured for the 4-port switch is approximately 2.7 dB and 3.6 dB at 1550 nm with a corresponding crosstalk less than 8 dB for the two TE modes, respectively. The payload transmission is also performed using both 10 Gb/s non-return-to-zero (NRZ) and 14.0625 Gbaud 4-level pulse-amplitude modulation (PAM4) pseudorandom binary sequence (PRBS)-31 data signal to analyze the performance of the switches. Clear open eyes are observed for both single-mode and simultaneous two-mode transmissions. The low insertion loss, low intermodal crosstalk over a large optical bandwidth, and the clear open eye validate the scalability of the proposed switches for larger port count and higher-order modes.**

***Index Terms*— Mode division multiplexing, multimode switches, optical switches, silicon photonics, wavelength division multiplexing.**

I. Introduction

THE advancement of silicon photonics (SiPh) technology in communication systems has been rising rapidly for over a decade. High integration density and low manufacturing cost due to compatibility with complementary metal-oxide-semiconductor (CMOS) established itself as a promising technology for the next generation optical networks. SiPh interconnects can provide large capacity, low latency, low power consumption, and high-speed data communication density within a small footprint in data center networks.

Switching and routing of data signals are one of the most basic requirements in data center networks. Wavelength division multiplexing (WDM) system is the most mature and widely used multiplexing technology in data centers. However, multiple laser sources are required to generate multiple WDM channels, which increase the power consumption and challenges on-chip system integration [1]. The capacity of data transmission over a limited optical bandwidth to meet the increasing demand is the main challenge of WDM systems. Mode division multiplexing (MDM) technology has attracted widespread attention by offering a new dimension to increase the data capacity using spatial modes of the waveguide using a single wavelength carrier [2]. Various SiPh devices have been developed to extend the capacity for MDM networks, such as mode multiplexer/de-multiplexer [3], switchable mode exchanger [4], multimode optical switches [5]–[12], power splitter [13], and more. Among them, multimode optical switch is a key component to route the multimode signals for MDM networks. Most of the proposed switches [9], [11], [12] depend on the demultiplexing-processing-multiplexing technique. De-multiplexing and multiplexing use to decode and encode the multimode signals to the fundamental mode signals and vice versa. Between these, single-mode optical switches are used to switch the signals for different outputs. This process is stable, but a large footprint and high power consumption are the bottlenecks of it. On the other hand, controlling several spatial modes simultaneously on a single waveguide is challenging due to the different structural relationships between the waveguide and the different modes. Recently, we have reported a balanced Mach–Zehnder interferometer (MZI) based 2×2 switch with a mode insensitive phase shifter for the first three quasi-transverse electric (TE) modes [10]. Multimode waveguide crossing [14] and multimode waveguide bending [15] have also been recently invented, allowing us to develop large port count multimode switches with direct multimode switching capability.

This letter experimentally demonstrates a novel design of mode insensitive 3-port and 4-port switches for the first two quasi-transverse electric (TE) modes that provide low insertion loss, intermodal crosstalk, and power consumption with a dynamic control by mode insensitive phase shifter. This letter is comprised of four sections. In section II, the design topology and building blocks are discussed. In section III, the experimental setup and the measurement results for these multimode switches are demonstrated. Finally, the summary with a brief analysis of these switches is presented in section VI.

II. Building Blocks and Design Topology

The proposed switches are designed for fabrication on a silicon-on-insulator (SOI) chip with a device thickness of 220 nm. The width of the waveguides for the fundamental mode (TE_0) and the two modes (TE_0 and TE_1) are 0.43 μm and 0.96 μm, respectively, as shown in Fig. 1(a). As depicted in Fig. 1(b), an adiabatic directional coupler-based mode multiplexer (MUX)/de-multiplexer (deMUX) is used for mode

Manuscript received January 12, 2021; revised April 1, 2021; accepted April 20, 2021. Date of publication April 27, 2021; date of current version May 5, 2021. This work was supported in part by the Canada Research Chair Program and in part by The Silicon Electronics-Photonics Integrated Circuits Fabrication (SiEPICfab) consortium. *(Corresponding author: Alok Das.)*

The authors are with the Department of Electrical and Computer Engineering, McGill University, Montreal, QC H3A 0E9, Canada (e-mail: alok.das@mail.mcgill.ca; guowu.zhang@mail.mcgill.ca; hassan.rahbardarmojaver@mcgill.ca; odile.liboiron-ladouceur@mcgill.ca).

Color versions of one or more figures in this letter are available at https://doi.org/10.1109/LPT.2021.3076096.

Digital Object Identifier 10.1109/LPT.2021.3076096

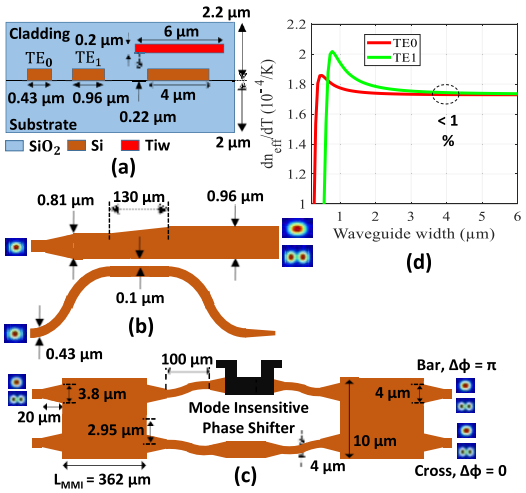

Fig. 1. (a) Waveguide cross-section of the fundamental mode (TE_0), two modes (TE_0,TE_1), and phase shifter; (b) schematic of the mode (de)multiplexer; (c) schematic of the mode insensitive MZI; (d) simulated dn_{eff}/dT as a function of the phase shifter width for the first two TE modes.

conversion at the input and output, respectively. The schematic diagram of a mode insensitive 2 × 2 MZI is shown in Fig. 1(c). All the parameters are optimized according to our previous work reported in [10]. The MZI consists of two 2 × 2 multimode interferometers (MMIs) connected by 4 μm wide Si waveguides with 100 μm long S-bend to prevent the thermal crosstalk induced by 200 μm long and 6 μm wide Titanium-tungsten (TiW) phase shifter placed between the two MMIs and 2 μm above one of the MZI balanced paths (Fig. 1(c)). The design of the mode insensitive phase shifter is accomplished by simulating dn_{eff}/dT for different TE modes as a function of the phase shifter's width as shown in Fig. 1(d). When the waveguide width is larger than 4 μm, the difference between the values of the dn_{eff}/dT for the two input TE modes is less than 1%. Thus, the mode insensitive phase shifter works for TE_0 and TE_1, simultaneously. The phase shifter remains mode insensitive for higher-order modes (e.g., TE_2, TE_3, etc) by increasing the width of the waveguide and the phase shifter. However, the heater's power consumption will increase in such case. For the first two input TE modes, the mode insensitive power consumption is measured around 40 mW per π-phase shift. All simulations are done using Lumerical tools.

The development of multimode switching topologies adds a new dimension of freedom for extended bandwidth. Conventional multimode switching matrices use the demultiplexing-processing-multiplexing technique, where processing works based on single-mode switching topology. Mode insensitive switch for higher-order modes is still challenging to realize due to large insertion loss and intermodal crosstalk induced by the complex building blocks such as multimode S-bend, waveguide crossing, and mode insensitive phase shifter. Thus, a large port count mode insensitive multimode switch for higher-order modes remains unavailable.

Our previous work investigated the 2 × 2 mode insensitive switch for the first three quasi-transverse electric modes, and it exhibits a good extinction ratio, bandwidth, reasonable insertion loss, and crosstalk [10]. It was observed that most of the insertion losses came from the mode MUX and deMUX. Thus, we optimize the mode MUX/deMUX by changing the length of the coupling region to achieve lower loss and

Fig. 2. Schematic of the proposed mode insensitive switch matrices; (a) 3 × 3 switch; (b) 4 × 4 switch.

crosstalk (Fig. 1(b)). In this design, we mitigate some of the loss and crosstalk for more scalable designs through the optimized MUX/deMUX designs and a layout avoiding waveguide crossings. Then, using the optimized 2 × 2 mode insensitive switch as a building block, we have designed the 3-port and 4-port mode insensitive switches for TE_0 and TE_1 modes for significantly improved performance (Fig. 2). Note that the crosstalk and bandwidth of these switches can be further improved using, for example, subwavelength-grating based mode MUX/deMUX and MMIs [16]. As multimode waveguide crossing has large insertion loss and intermodal crosstalk [14], thus we utilize the 2 × 2 MZI to avoid conventional multimode waveguide crossing. After further optimization of the building blocks for higher-order modes (such as TE_2, TE_3, TE_4, etc.), the Spanke-Beneš switching topology [17] can be scaled to higher-order modes and large port count, simultaneously. This demonstration opens the door to realize large port count and higher order modes.

The proposed SiPh switches are designed for an SOI wafer through Applied Nanotools Inc. (ANT) [18]. The device footprint of the 3-port and 4-port mode insensitive switches are 4.5 mm × 0.5 mm and 5 mm × 1 mm, respectively.

III. Experimental Results

Both continuous wave (CW) and payload transmission measurements have been done to characterize the switches.

A C-band tunable laser is used to perform the CW measurements. At the output of this laser source, a polarization controller (PC) is connected to maintain the on-chip polarization of the optical signal to a quasi-TE optical mode. At the output of the chip, a power meter is connected to measure the optical power. The CW measurements are normalized to the grating couplers' losses.

Fig. 3 shows the corresponding spectrum response for the 3-port mode insensitive switch at 1550 nm. For TE_0 and TE_1 modes, the lowest insertion loss (IL) measured 1.8 dB and 2.4 dB, respectively at I3-O3 where only one MZI building block is employed, and the highest insertion loss is 2.6 dB and 3.3 dB for TE_0 and TE_1, respectively, where two MZIs are present. The crosstalk (XT) is less than 10 dB and 8 dB for TE_0 and TE_1 modes, respectively, within the 40 nm of bandwidth (BW) range from 1530 to 1570 nm.

The corresponding spectrum responses for the 4-port mode insensitive switch are shown in Fig. 4. The lowest (highest) insertion loss measured for TE_0 and TE_1 are 2 dB (2.7 dB) and 2.6 dB (3.6 dB), respectively, at 1550 nm. After using the multiple stages of cascaded MZI, the crosstalk is measured at most 8 dB for both TE_0 and TE_1 modes, within the 40 nm wavelength range from 1530 to 1570 nm.

Payload transmission is then experimentally performed to demonstrate the switching performance for real data transmission system (Fig. 5). To observe the impact of intermodal crosstalk, we divide this experiment into two parts. In the

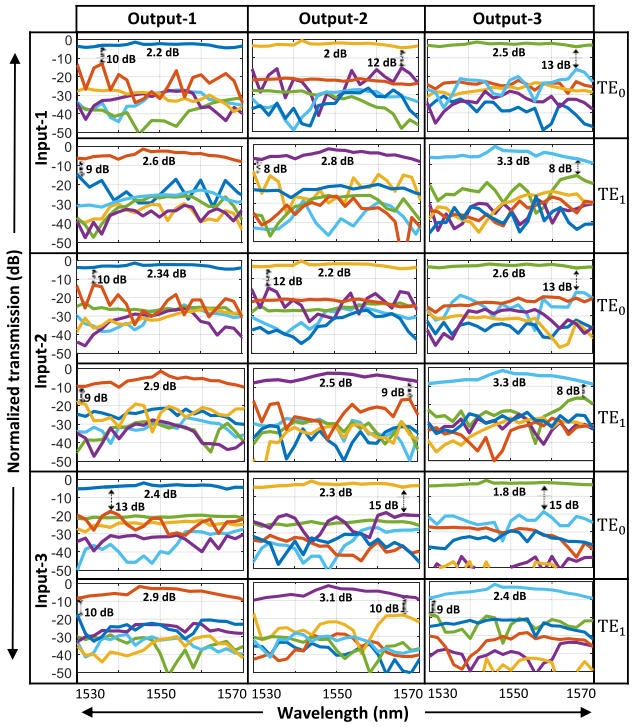

Fig. 3. Measured transmission spectrum for both modes (TE_0 and TE_1) as a function of wavelength for the 3 × 3 mode insensitive switch.

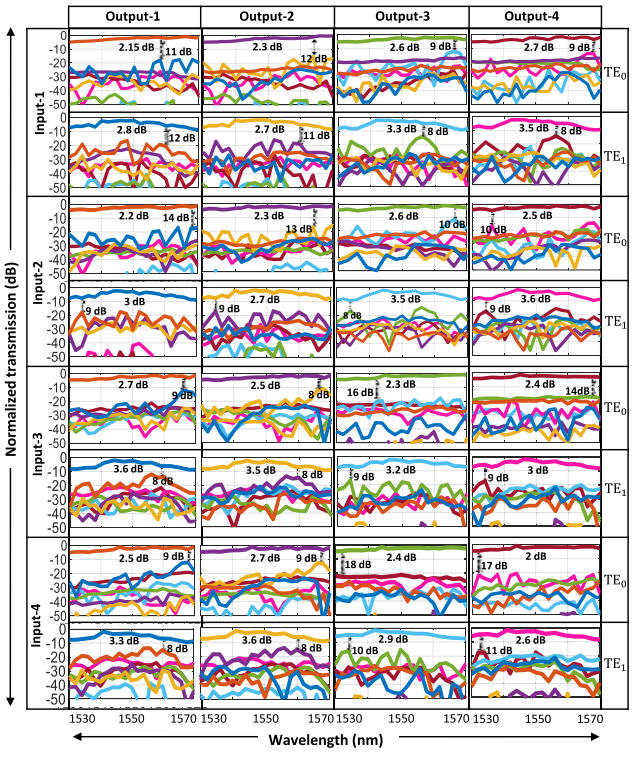

Fig. 4. Measured transmission spectrum for both TE_0 and TE_1 modes as a function of wavelength for the 4 × 4 mode insensitive switch.

first part, we transmit only one mode, and in the second part, both TE_0 and TE_1 modes are transmitted simultaneously to understand the system impact of modal crosstalk.

The output of the C-band tunable laser is connected to a modulator with 12.3 GHz and 40 GHz 3-dB RF bandwidth for NRZ and PAM4 data signals, respectively, through a

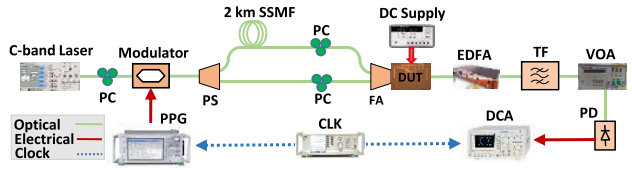

Fig. 5. Experimental setup of the switch (DUT) for real data transmission. PC: polarization controller; PS: power splitter; SSMF: standard single-mode fiber; FA: fiber array; TF: tunable filter; EDFA: erbium-doped fiber amplifier; CLK: clock synthesizer; DCA: digital communication analyzer; VOA: variable optical attenuator; PPG: pulse pattern generator.

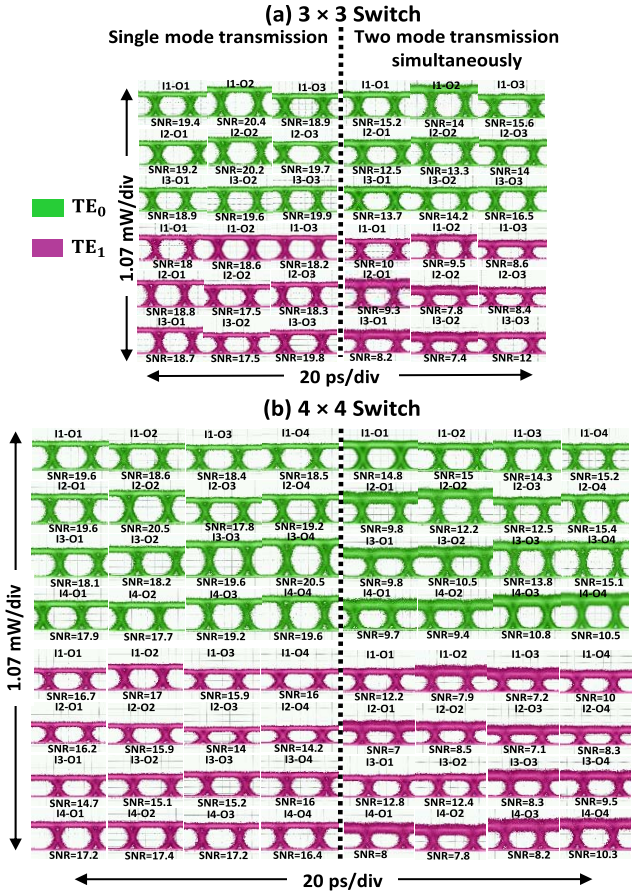

Fig. 6. Eye diagrams using 10 Gb/s NRZ PRBS-31 signal for both single-mode and two-mode simultaneous transmission; (a) 3 × 3 switch; (b) 4 × 4 switch.

polarization controller (PC). The 1550 nm CW signal is modulated by a 10 Gb/s NRZ or 14.0625 Gbaud PAM4 PRBS-31 signal from a pulse pattern generator (PPG). The modulated signal then goes through a 1 × 2 power splitter to generate two-channel signals. One channel is delayed by passing through a 2 km standard single-mode fiber (SSMF) to decorrelate the signals. Then the signals passed through another PC to the DUT (device under test), where light is coupled with a grating coupler. The output signal is amplified by an erbium-doped amplifier (EDFA) to compensate for the device's insertion loss. Then it passes through a C-band tunable filter to reduce the unwanted amplified spontaneous emission (ASE) noise generated by the EDFA. A variable optical attenuator (VOA) is used to maintain the optical power to the photodetector's (PD) desired level. After the PD, the RF signal is fed to a digital communication analyzer (DCA) to capture the eye

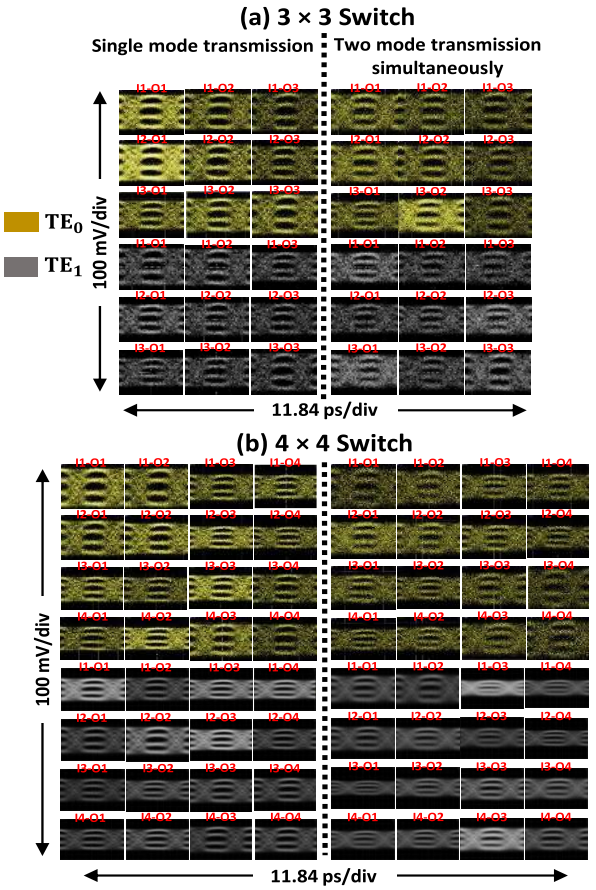

Fig. 7. Eye diagrams using 14.0625 Gbaud PAM4 PRBS-31 signal for both single-mode and two-mode simultaneous transmission; (a) 3 × 3 switch; (b) 4 × 4 switch.

TABLE I

SUMMARY OF THE EXPERIMENTAL RESULTS AT 1550 nm

Switch	Mode	IL (dB)	XT (dB)	Worst SNR (NRZ)		Power (pJ/bit)
				1-mode	2-mode	
3 × 3	TE_0	2.6	10	18.9	12.5	2
	TE_1	3.3	8	17.5	7.5	
4 × 4	TE_0	2.7	8	17.7	9.4	2.5
	TE_1	3.6	8	14	7	

diagram. A synthesized clock (CLK) synchronizes the PPG and the DCA.

Eye diagrams are measured for 3-port and 4-port switches using both the 10 Gb/s NRZ (Fig. 6) and 14.0625 Gbaud PAM4 (Fig. 7) PRBS-31 signals at 1550 nm. For single-mode transmission, clear open eyes are observed. However, the eye diagrams are deteriorated in simultaneous transmission owing to the intermodal crosstalk. The TE_1 mode suffers much from the deterioration because of higher insertion loss and crosstalk. The worst crosstalk for TE_1 is 18 dB and 14 dB at 1550 nm for 3-port and 4-port switch, respectively. However, in all the cases, a clear open eye is measured with reasonable signal-to-noise ratio (SNR), which confirms the operation of these switches in MDM networks.

Table I summarizes experimental results for these mode insensitive switches within 40 nm of bandwidth range from 1530 nm to 1570 nm.

IV. CONCLUSION

In this letter, we propose and experimentally demonstrate a novel design for a 3-port and 4-port two-mode switching matrices. The mode insensitive heater enables switching simultaneous performance on two modes and reduces the overall switch power consumption. If all the switching channels are active, the total power (energy) consumption for the 3-port and 4-port thermal switches are approximately 120 mW (2 pJ/bit) and 200 mW (2.5 pJ/bit), respectively. Both switching matrices exhibit low insertion loss and intermodal crosstalk over 40 nm of bandwidth range. The clear open eyes and good SNR show evidence that these switches are fully compatible with low-noise data transmissions in MDM systems. The scalable switching topology and existing building blocks show the potentials to design larger switching matrices with a greater port count, even for the higher-order modes.

REFERENCES

[1] D. Dai, J. Wang, and Y. Shi, "Silicon mode (de) multiplexer enabling high capacity photonic networks-on-chip with a single-wavelength-carrier light," *Opt. Lett.*, vol. 38, no. 9, pp. 1422–1424, 2013.
[2] B.-T. Lee and S.-Y. Shin, "Mode-order converter in a multimode waveguide," *Opt. Lett.*, vol. 28, no. 18, pp. 1660–1662, 2003.
[3] H. Shu, B. Shen, Q. Deng, M. Jin, X. Wang, and Z. Zhou, "A design guideline for mode (DE) multiplexer based on integrated tapered asymmetric directional coupler," *IEEE Photon. J.*, vol. 11, no. 5, pp. 1–12, Oct. 2019.
[4] C. Sun, Y. Yu, G. Chen, and X. Zhang, "Integrated switchable mode exchange for reconfigurable mode-multiplexing optical networks," *Opt. Lett.*, vol. 41, no. 14, pp. 3257–3260, Jul. 2016.
[5] B. Stern *et al.*, "On-chip mode-division multiplexing switch," *Optica*, vol. 2, no. 6, pp. 530–535, Jun. 2015.
[6] Y. Xiong, R. B. Priti, and O. Liboiron-Ladouceur, "High-speed two-mode switch for mode-division multiplexing optical networks," *Optica*, vol. 4, no. 9, pp. 1098–1102, Sep. 2017.
[7] R. B. Priti and O. Liboiron-Ladouceur, "Reconfigurable and scalable multimode silicon photonics switch for energy-efficient mode-division-multiplexing systems," *J. Lightw. Technol.*, vol. 37, no. 15, pp. 3851–3860, Aug. 1, 2019.
[8] Y. Zhang, Y. He, Q. Zhu, C. Qiu, and Y. Su, "On-chip silicon photonic 2 × 2 mode and polarization-selective switch with low inter-modal crosstalk," *Photon. Res.*, vol. 5, no. 5, pp. 521–526, 2017.
[9] H. Jia, T. Zhou, L. Zhang, J. Ding, X. Fu, and L. Yang, "Optical switch compatible with wavelength division multiplexing and mode division multiplexing for photonic networks-on-chip," *Opt. Exp.*, vol. 25, no. 17, pp. 20698–20707, 2017.
[10] G. Zhang, H. R. Mojaver, A. Das, and O. Liboiron-Ladouceur, "Mode insensitive switch for on-chip interconnect mode division multiplexing systems," *Opt. Lett.*, vol. 45, no. 4, pp. 811–814, 2020.
[11] Y. Zhang, R. Zhang, Q. Zhu, Y. Yuan, and Y. Su, "Architecture and devices for silicon photonic switching in wavelength, polarization and mode," *J. Lightw. Technol.*, vol. 38, no. 2, pp. 215–225, Jan. 15, 2020.
[12] L. Yang *et al.*, "General architectures for on-chip optical space and mode switching," *Optica*, vol. 5, no. 2, pp. 180–187, Jun. 2018.
[13] Y. Luo, Y. Yu, M. Ye, C. Sun, and X. Zhang, "Integrated dual-mode 3 dB power coupler based on tapered directional coupler," *Sci. Rep.*, vol. 6, no. 1, p. 23516, Sep. 2016.
[14] S. H. Badri, H. Rasooli Saghai, and H. Soofi, "Multimode waveguide crossing based on a square Maxwell's fisheye lens," *Appl. Opt.*, vol. 58, no. 17, pp. 4647–4653, Jun. 2019.
[15] H. Wu, C. Li, L. Song, H.-K. Tsang, J. E. Bowers, and D. Dai, "Ultra-sharp multimode waveguide bends with subwavelength gratings," *Laser Photon. Rev.*, vol. 13, no. 2, Feb. 2019, Art. no. 1800119.
[16] L. Xu *et al.*, "Ultra-broadband and compact two-mode multiplexer based on subwavelength-grating-slot-assisted adiabatic coupler for the silicon-on-insulator platform," *J. Lightw. Technol.*, vol. 37, no. 23, pp. 5790–5800, Dec. 1, 2019.
[17] R. A. Spanke and V. E. Benes, "N-stage planar optical permutation network," *Appl. Opt.*, vol. 26, no. 7, p. 1226, Apr. 1987.
[18] *Applied Nanotools*. Accessed: Oct. 5, 2020. [Online]. Available: https://www.appliednt.com